Published online in 2010 as part of U.S. Geological Survey Scientific Investigations Report 2010-5091.

Acoustic Gravel-Momentum Sensor

John Downing

Port Townsend, Washington, United States

Abstract

The development of acoustic devices for measuring gravel momentum is described and laboratory tests of a gravel-transport sensor in a moving-bed flume and a field trial in a California stream with a weighing-trap bedload monitor are presented. The gravel-transport sensor consists of a steel pressure plate, bonded to polyvinylidene fluoride film, which is mounted on an aluminum block. When gravel collides with the plate, it generates an electric charge proportional to the impact force and the integral of the charge is proportional to the momentum of the particles. The shape, amplitude, and duration of impact signals from spheres made from a variety of materials such as stone, glass, steel, or tungsten carbide did not correlate with particle mass. Estimating particle mass from signal properties therefore appears unlikely. The GTS transducer has been configured for hand-held operation like a Helley-Smith sampler and as an embedded, self-recording instrument. The mass transport as bedload is calculated from the product of digital counts, which are proportional to momentum, and a conversion factor, divided by the sum of the size-fraction-weighted grain velocities. The conversion factor is instrument specific and the bedload size distribution must be known and must remain the same during transport events. Analysis of video images acquired in the flume indicated that efficiencies range from 20 to 40%. Efficiency is the percentage of momentum of particles moving toward a GTS transducer that it actually measures. The flume tests indicated that efficiency is not correlated with particle size and that fast-moving particles in the bedload contribute more to the measured momentum than slow-moving ones.

KEYWORDS: Gravel bedload, acoustics, particle-momentum sensor

1. Introduction

The idea of using acoustic signals generated when entrained particles strike a rigid object for sediment-transport research is not new. Forty years ago Sharp and O'Neill (1968) reported the use of a wire to detect sediment flowing in pipes, and 13 years later Downing (1981) reported a similar technique for measuring sand bedload in a stream and in the swash zone, (Fig. 1). In the early 1990's this approach was extended to measure gravel bedload with a pipe containing an acoustic detector and recording electronics (Downing, 1993). Both devices were essentially impact counters that could provide continuous digital records of the onset and cessation of bedload as well as its relative intensity. If the particle-size distribution, sediment density and counter efficiency (the percentage of particles

moving toward the sensor that actually hit it), were known, one could estimate bedload transport in kg m^{-1} s^{-1} from the size-weighted ping rate. Here I describe further developments of acoustic devices for measuring gravel momentum and present the results of laboratory tests in a moving-bed flume and a field trial in a California stream, where a weighing-trap bedload monitor installed by the U.S. Forest Service, has been in operation since 1962.

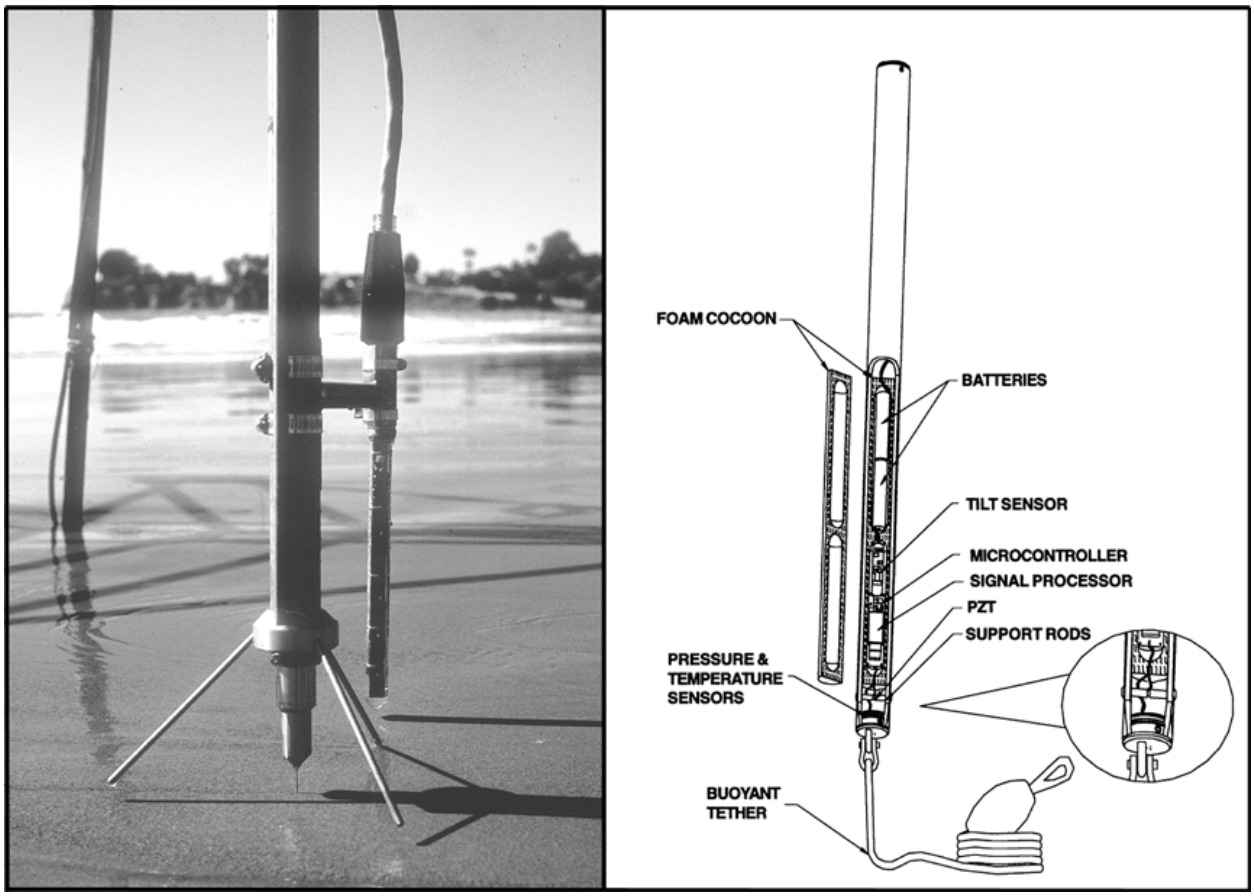

Figure 1. Impact sensors for sand (left) and gravel (right) bedload.

2. Sensor Description

The gravel-transport sensor (GTS) consists of a 1.6-mm, stainless steel pressure plate bonded to polyvinylidene fluoride (PVDF) film, which is mounted on an aluminum block; see the exploded views of the GTS assemblies shown in Fig. 2. When gravel collides with the plate, it compresses the PVDF film and generates an electric charge proportional to the force exerted on it. The electric charge is converted to voltage by a charge amplifier. Fig. 3 shows waveforms generated by impacts of spheres made of stone, glass, steel, and tungsten carbide. A typical impact signal has a major positive voltage peak followed by a minor one. The integral of the impact force is proportional to the momentum of the impacting particles and therefore the voltage-time integral of an impact signal in V s^{-1} is a direct measure of particle momentum. Polyvinylidene fluoride film is used because of its high sensitivity, excellent formability, and low mechanical quality (it is acoustically "dead"), elastic modulus (< 1% of

aluminum), and cost. Transducers constructed in this way are sensitive to particle momentum in the range from 0.00002 (a 5-mm stone moving at 0.12 m s^{-1}) to 0.08 kg m s^{-1} (a 100-mm stone moving at 0.06 m s^{-1}). Submerged GTS transducers are calibrated with steel spheres falling at terminal velocity to determine the formula for converting impulse to momentum; see sample calibration plot (Fig. 4).

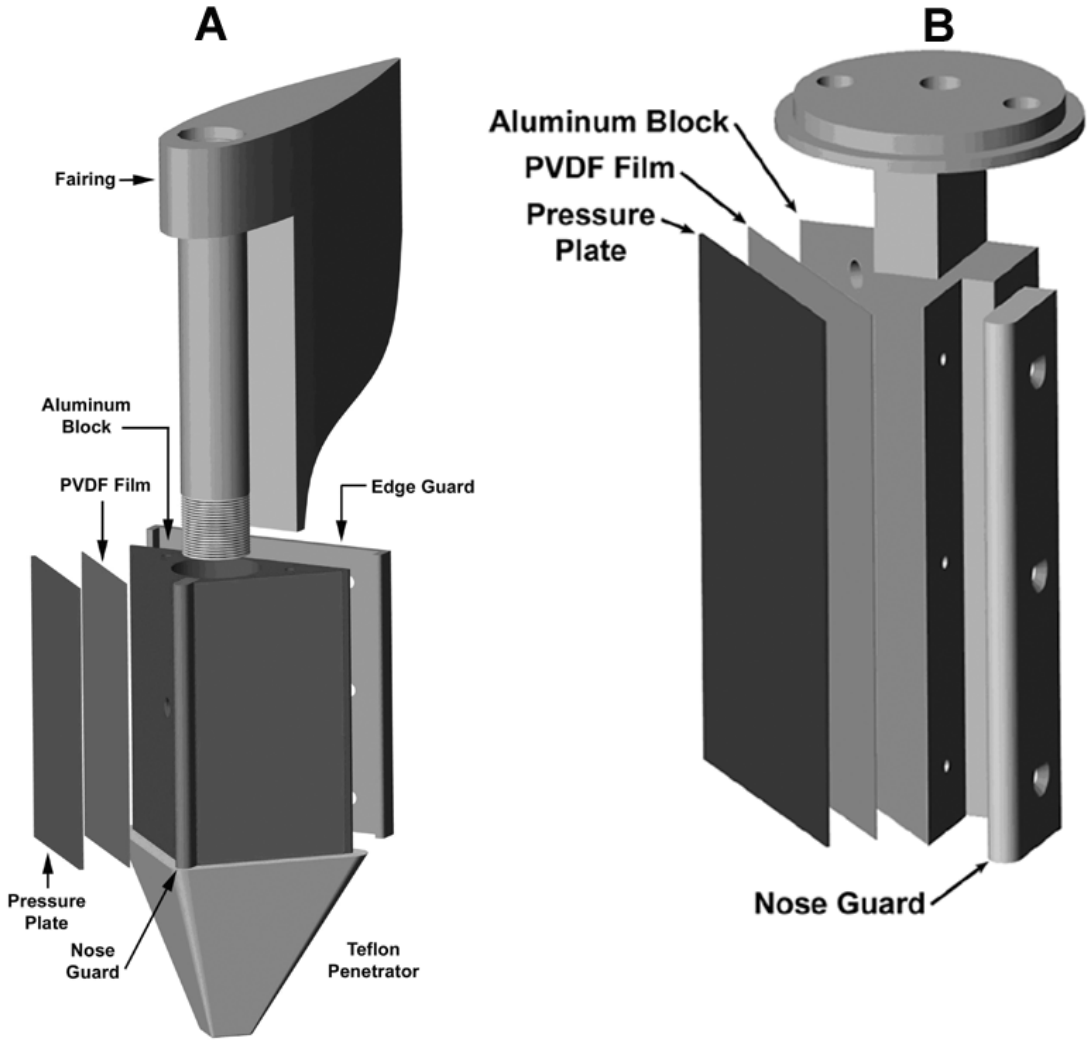

Figure 2. GTS- I (A) and GTS-II (B) Gravel-transport sensors.

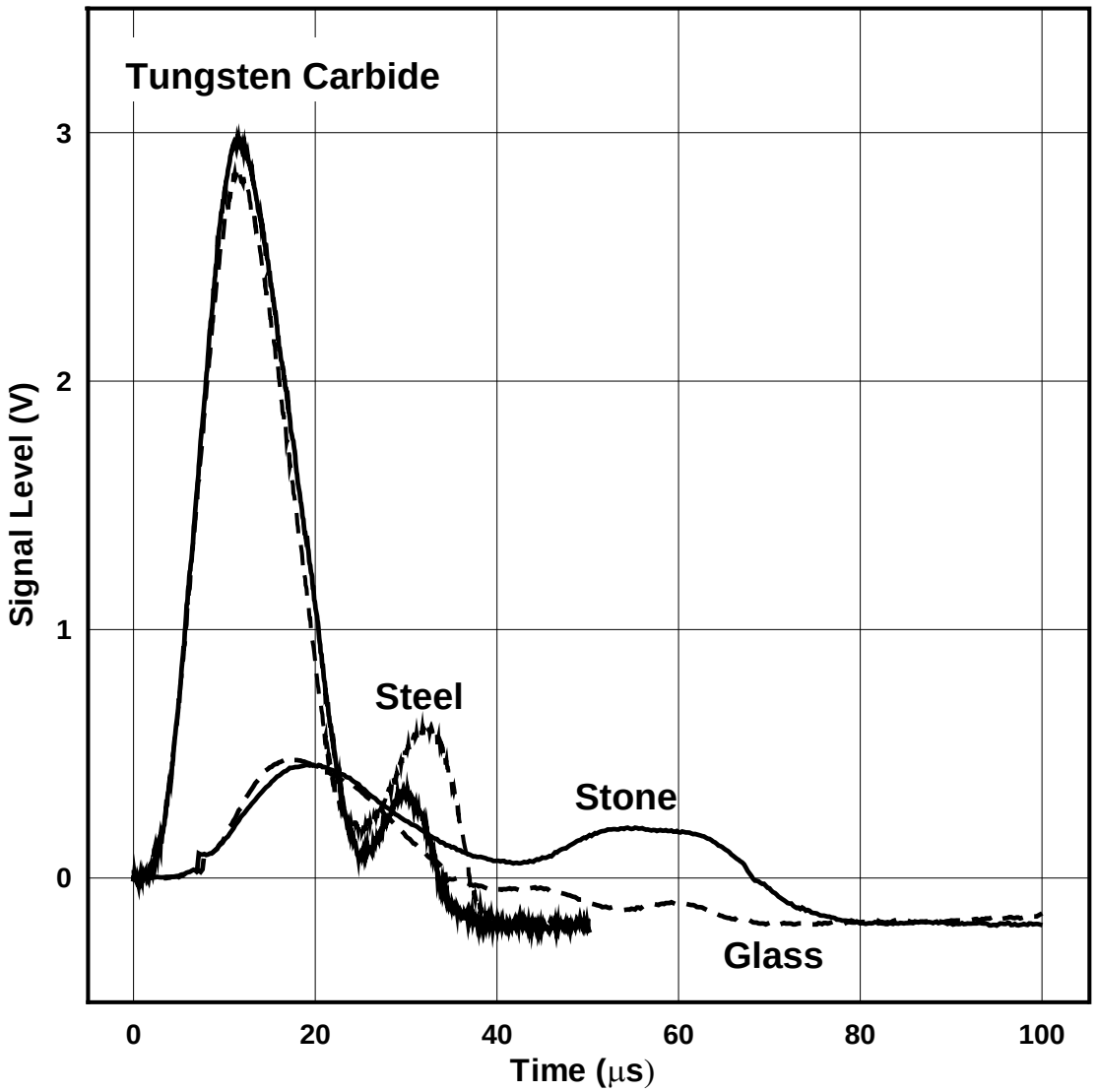

Figure 3. Waveforms for tungsten carbide, steel, stone and glass spheres.

The GTS transducer is configured for hand-held operation (GTS-I, Fig. 2) with a drag-reduction fairing. The sensor has two 54 by 105-mm PVDF elements bonded to an anodized, 7075-T6 aluminum support in a 90°, open-book configuration. The exposed edges are protected from impact damage with steel guards. The open-book geometry gives an angle between particle trajectories and the pressure plate of 45° and cross-flow width of 76 mm. During sampling, the operator positions the GTS-I at a sampling location; pushes the penetrator into the streambed; and switches the logger on to record bedload momentum. The process is repeated at several points across the channel and the logger is switched off between stations. The second application (GTS-II) is an embedded sensor mounted on an anchor assembly containing batteries, electronics, and the data logger. The construction of the sensor is similar to the GTS-I except that a single PDVF element is used.

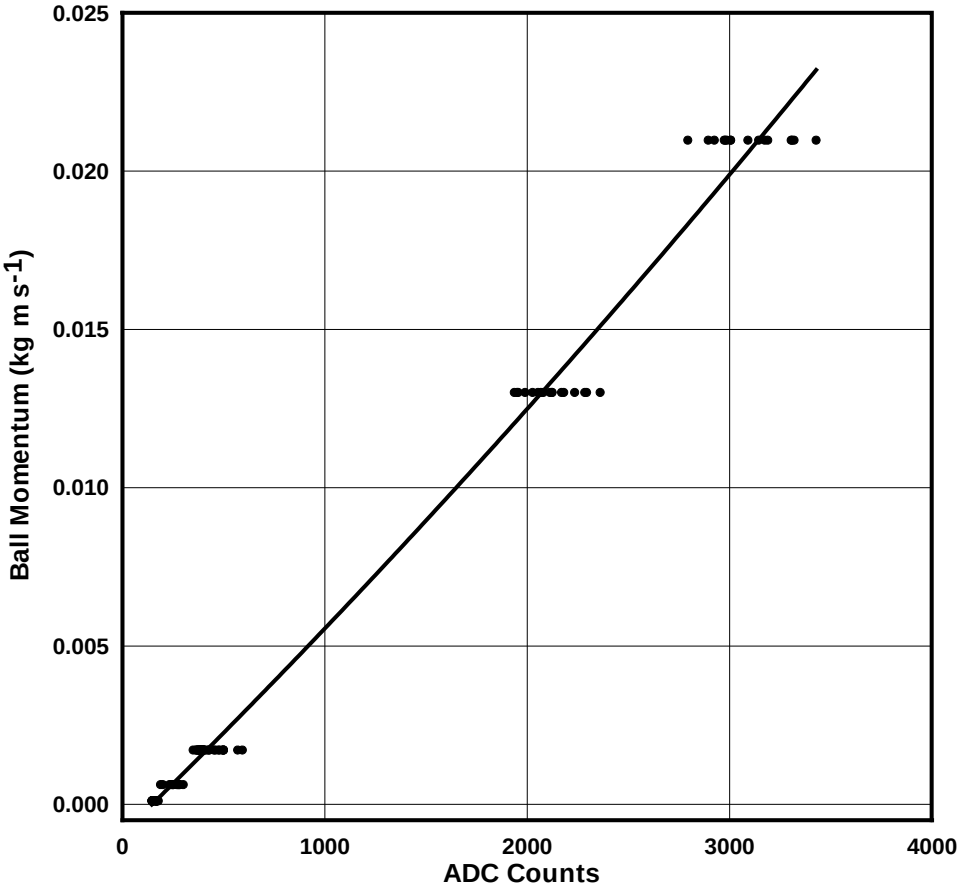

Figure 4. Sample calibration of GTS-II system.

2.1 Signal Processing

The electronics incorporate an analog signal processor, a microcontroller and a solid-state data memory. Signals from the acoustic detector are input to a charge amplifier and high-pass filter that removes low-frequency noise from flow turbulence, hydrostatic pressure fluctuations, bedload noise, etc. The signal processor: 1) detects threshold exceedance with variable-gain amplification to compensate for transducer sensitivity; 2) triggers pulse integration, timing, and counting and 3) signals the microprocessor to record integrator, timer, and counter outputs. The impact-pulse areas are converted to digital counts by the signal processor. A 300-hour record of bedload transport with 60 records per hour and a maximum impact rate of 90 Hz can be logged in the solid-state memory. The GTS-II system also has a pressure transducer for measuring depth along with momentum data. A submerged GTS transducer is calibrated by dropping steel spheres onto the pressure plate from heights sufficient to produce terminal fall velocities. The sphere size is varied to produce the desired range of momentum (see Fig. 4). Life-cycle testing demonstrated that GTS transducers can withstand the impacts of 340,000 20-mm stones moving at 0.4 m s^{-1} with only cosmetic damage. Moreover, GTS II transducers operated reliably for 20 transducer months in streams where 264 hours of transport occurred.

GTS systems log records of particle momentum that can be converted to mass transport with a method formulated on fractional particle speeds, settling and critical-shear velocities, and bed shear stress. The critical shear stress is computed by the recipe explained in Section 4. Settling velocities can

be computed with several published formulas. The bed shear stress is estimated from the local bed slope and water depth. Once the velocities are known from stream hydraulics, the mass transport as bedload is computed by dividing momentum by size-weighted particle velocity. An inherent assumption of the method, which must be verified for GTS applications, is that the size distribution of the bedload is known and remains the same during transport events.

2.2 Waveform Properties

Early in the GTS development, a feasibility study was conducted to determine if particle mass could be extracted in some way from waveform properties such as pulse morphology, duration, asymmetry, etc. Several properties of the particles and their interaction with the GTS during an impact were considered. The dynamic response of the GTS transducer during an impact is influenced by the elastic modulus, damping and the impedance of a connected electrical load. Because the load impedance effect was removed by minimizing wave distortion and oscillations of the circuit, the dynamic response of the transducer is determined mainly by the elastic modulus of the PVDF film and the elastic interaction of the particle with the pressure plate. This interaction is characterized by the coefficient of restitution, ε, which equals $(h/H)^{1/2}$, where H and h are the fall and rebound distances associated with a free-falling particle. The ε coefficients of the test spheres were determined by dropping them on the transducer in air and measuring h and H on video images. The spheres were selected to have similar masses (13.7 to 17.2 g) and a range of elastic moduli (65 to 720 GPa) and ε values (0.72 to 0.87). Table 1 summarizes the material properties and sphere dynamics. The waveforms for underwater impacts were recorded in a deep water tank where terminal velocities could be achieved and measured on video images. Impact signals were logged with a Fluke recording oscilloscope for five replicate drops of each test sphere.

Table 1. Material properties of spheres used in waveform tests and some waveform properties.

	ρ	D	Mass	W_s	P	Modulus	ε	T_p	Area
	g cm^{-3}	mm	g	m s^{-1}	kg m s^{-1}	Gpa		µs	V µs
Stone	2.50	23.00	17.20	1.0	0.017	65	0.72	68	0.55
Glass	2.50	22.00	13.70	1.0	0.014	51	0.87	31	0.57
Stainless Steel	8.00	16.00	14.50	1.7	0.024	193	0.80	22	2.74
Tungsten Carbide	15.00	12.70	15.00	2.0	0.030	720	0.74	24	2.70

Fig. 3 shows the waveforms from the various sphere materials. The waveform for the stone sphere has major and minor peaks with an amplitude ratio of about 1.6, whereas the steel and tungsten carbide spheres, with high elastic modulus and low ε values, produce a dominant peak, followed by a secondary one with amplitude ratios ranging from ~ 4.2 to 6.5. The waveform for glass has a single dominate peak. Stone spheres produce peaks that persist two times longer than those produced by the other materials. While the peak morphologies and ε values for different materials are distinctive, no clear relationships among waveform shapes, peak durations, ε values, and particle mass could be delineated and it was concluded that direct estimates of particle mass will not be easily obtained from waveform characteristics.

3. Flume Tests

The field data from bedload measurements are notorious for confounding environmental factors, such as the high spatial and temporal variability of transport, with the imprecision of bedload traps and the unknown accuracy of concurrently tested equipment (Downing et al., 2003). In Little Granite Creek for example, the standard error of the ratios of transport measured with Bunte traps (Bunte et al., 2003) separated by one meter was 78% and in the Piedra River, the standard error of paired transport rates measured with Elwha bedload samplers was 57%. In order to have more control over these factors, testing was conducted in a re-circulating, tilting-bed water flume at Colorado State University (CSU) with small (D_{50} = 13 mm), medium (D_{50} = 23 mm), and large (D_{50} = 30 mm) gravel. Size was determined by image analysis. An average stone density of 2600 kg m^{-3} was determined by direct measurements of sediment mass and volume. Histograms of the particle speed and direction for the medium-size gravel used in the flume are shown in Fig. 5.

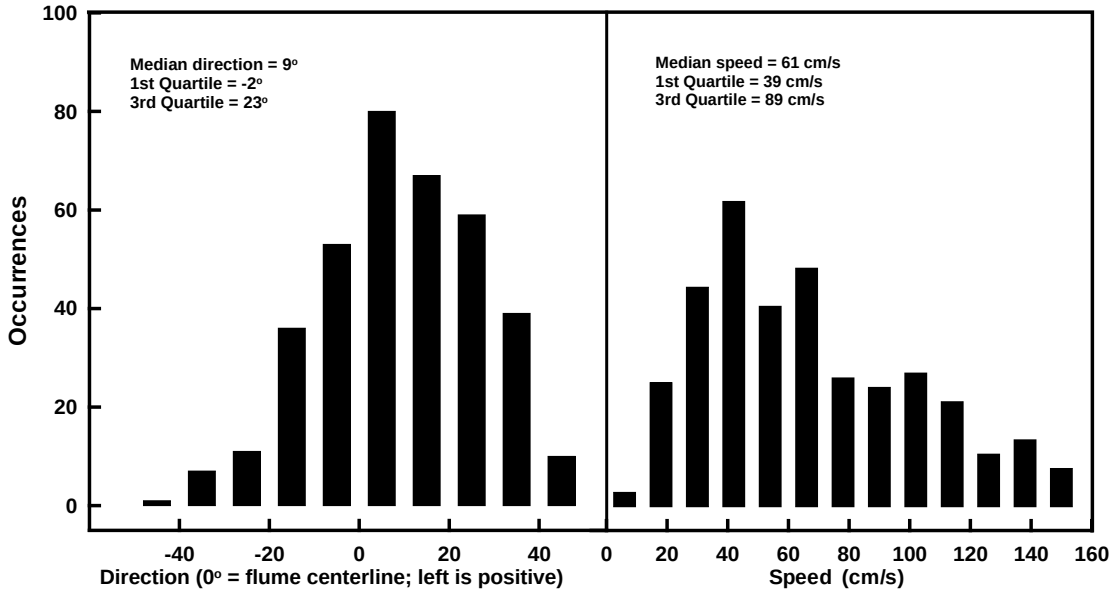

Figure 5. Medium-gravel velocity statistics.

The CSU flume is 18 m long, 0.6 m wide and can produce 0.5-m flow depths. For the tests reported here, the mean flow depth at the GTS transducer was set to ~0.25 m and the average flow velocity was 1.75 m s^{-1}. The test section and GTS with video camera are shown in Fig. 6. The base of the pressure plate was set 5 cm below the gravel-bed surface to ensure that the transducer was exposed to moving gravel at all times. The testing procedures involved recording synchronous GTS records and video images of the base of the GTS transducer where gravel impacts occurred. The scene in front of the transducer was recorded with an underwater video camera that was bolted to the top of the transducer. A pin-hole "spy camera" was used in order to get a wide-angle view with a short focal length. The spatial resolution is ± 0.14 mm. The frame rate was 30 Hz, giving time and velocity resolutions of 33 ms and 0.004 m s^{-1}, respectively. The GTS controller was set to record one-second averages of digital counts. A total of 203,400 frames were recorded during transport events when about 13,000 stones passed through the measurement area and about 3,000 of them impacted the GTS.

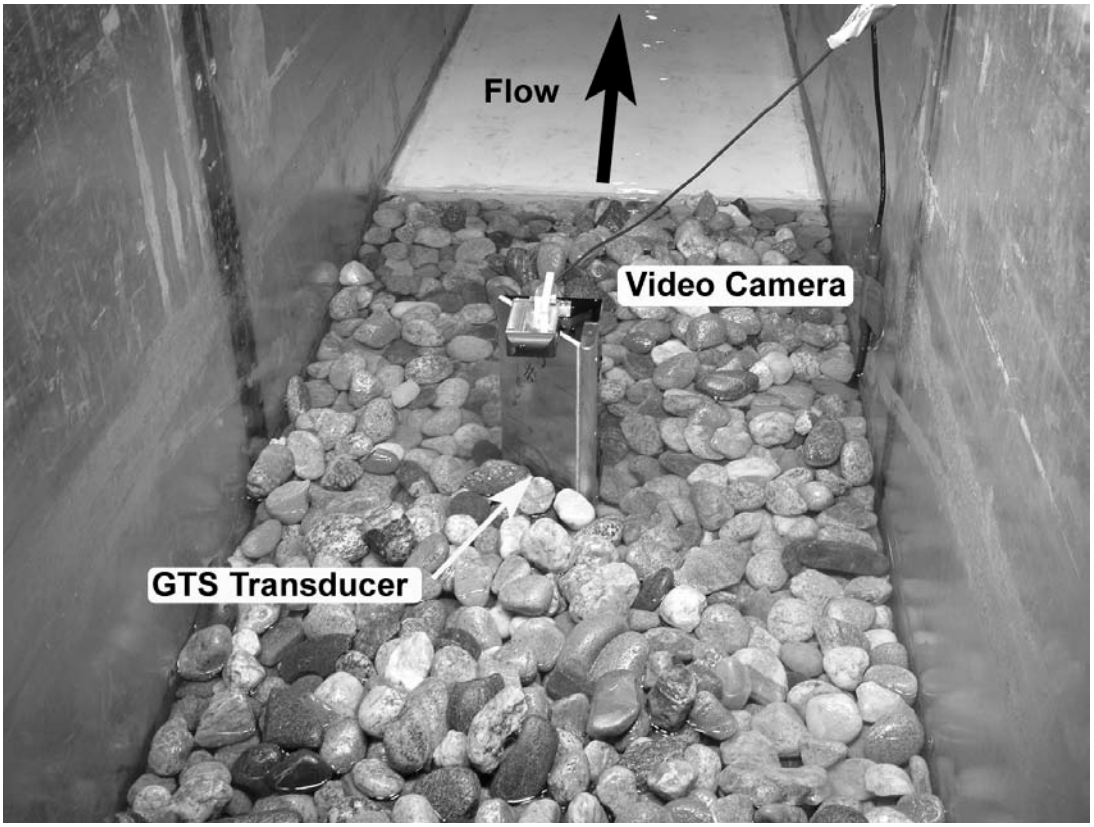

Figure 6. Test bed, GTS installation, and video camera position in flume.

3.1 Flume Results

Fig. 7 shows a sample of eight consecutive video images of conditions in front of the GTS pressure plate during a transport event (particles of interest are highlighted and labeled A through F). Several key interactions between gravel particles and the pressure plate are illustrated in the images. Particle ‘A’ hits the plate twice before it is swept past the GTS, while particles ‘B’ and ‘E’ hit only once. Particles ‘C’ and ‘D’ move past the sensor without hitting it. Particle ‘F’ moves upstream without contacting the plate.

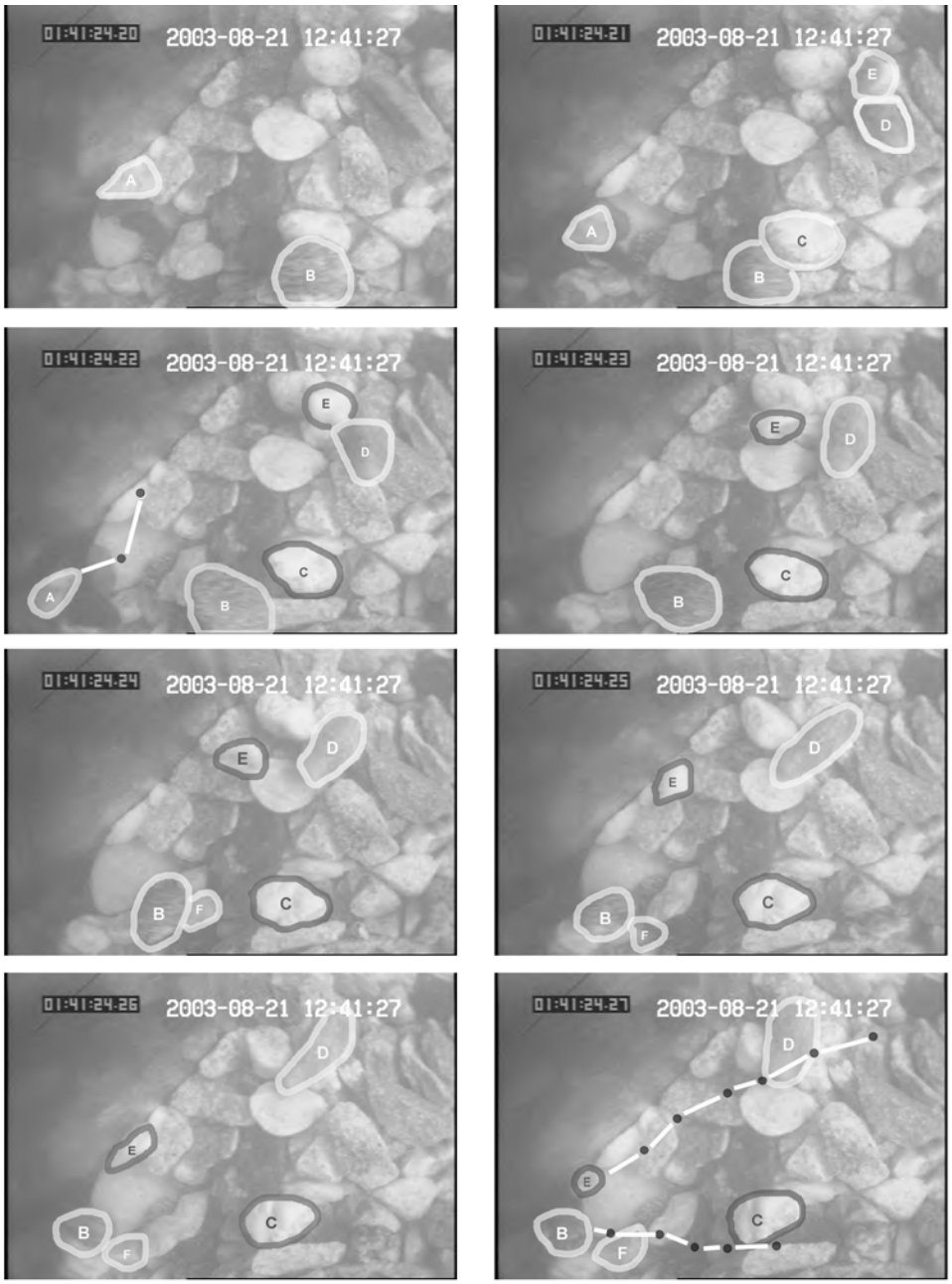

Figure 7. Underwater images of moving gravel particles. The frame rate is 30 per second and the frame number is the last two digits in the left-hand display.

Table 2 lists the quartiles of particle size (D), velocity (V_p), and direction (ϕ). In general, the median particle speeds are higher than would be expected for a flat bed because slow-moving particles tend to be swept around the mound in front of the transducer and do not contribute as much to the observed velocities. On the speed and direction histograms (Fig. 5), positive directions and higher speeds correspond to motion in the left hand quadrant, toward the left wall seen by an observer looking downstream. They show that gravel velocity is influenced by the flow around the GTS transducer, which is amplified by the 45° angle of the pressure plate. As particles approach the transducer, they are more likely to be deflected to the pressure-plate side as is indicated by the speed and direction statistics

shown on Fig. 5. The speed bias is reflected in the positive skewness, $(V_{25} + V_{75} - 2V_{50})/2$, of small stone speeds (+ 12.5 cm s^{-1}), medium stones (+ 3 cm s^{-1}), and large stones (+ 3.5 cm s^{-1}). The velocity bias results in lower gravel momentum than would be measured without flow disturbance.

Table 2. Summary of bedload size and velocities in CSU flume.

	D_{25} mm	D_{50} mm	D_{75} mm	V_{25} cm s^{-1}	V_{50} cm s^{-1}	V_{75} cm s^{-1}	φ_{25}	φ_{50}	φ_{75}
Small	10.7	13.4	15.2	60	90	115	-4^o	3^o	9^o
Medium	18.2	21.4	24.9	39	61	89	-2^o	9^o	23^o
Large	33.2	40.0	45.7	40	59	85	-7^o	10^o	19^o

Transducer efficiency is the ratio of measured momentum to the momentum of particles moving toward the transducer expressed as a percentage. The horse vortex and stagnation area in front of the transducer produce a scour crater with a mound that diverts some particles around the transducer and prevents them from contacting the pressure plate. Efficiency was evaluated for the trajectories of 410 small, 311 medium, and 120 large particles to determine what percentage of them actually struck the pressure plate. The efficiencies listed in Table 3 were 21%, 37%, and 24% for small, medium, and large gravel, respectively. These differ from 100% by comparable amounts determined for bedload traps. Also, video images show that fast-moving particles are more likely to climb the mound and strike the pressure plate than slower ones, which tend to roll around the mound and miss the transducer. The shielding effect produces a bias toward faster particles, because they are more likely to be sampled and to contribute momentum measurements than slow ones.

The output of the signal processor is the average impact-pulse area converted to digital counts, which when multiplied by the impact count, represents the total momentum of impacts that occur during a sampling interval. The actual momentum delivered to the transducer measured by image analysis over the same time interval divided by the digital counts is the conversion factor for the transducer under the tested conditions. These values indicate the number of digital counts that will be indicated per unit of momentum delivered to the transducer. The mass transport producing the delivered momentum must be determined with an independent estimate of velocity as discussed in Section 4. The conversion factors and efficiencies determined in this way are given in Table 3.

Table 3. Summary of flume results.

Event	Duration (hours)	Mass (kg)	Ave. Qb (kg m^{-1} h^{-1})	P (kg m/s)	Counts (X 10^{-6})	CF (X 10^{7})
Event-1 (12/13-17/2002)	58	26.8	4.62	9.26	22.80	4.06
Event-2 (12/27-31/2002)	59	122	20.7	n.d.	n.d.	n.d.
Event-3 (1/12-13/2003)	40	73.5	18.4	27.80	58.10	4.79
Total transport hours	**157**					

4. Field Trials

The hydraulic features of the North Fork of Caspar Creek are: channel width = 4.4 m; mean depth = 0.5 m; local bed slope = 0.0038; bankfull flow = 2.3 m3 s-1; mean velocity = 1.03 m s-1 and D50 of the surface sediment = 9 mm. Fig. 8 shows the hydrograph for Caspar Creek during the bedload events reported here. Two GTS systems and support instrumentation were operated at the site during

water years WY2002 and WY2003 in conjunction with Birkbeck weighing bedload traps. Weighing traps are the most accurate direct sampling device in use today, and in 2002, the Caspar Creek traps were the closest operating ones in the U.S.

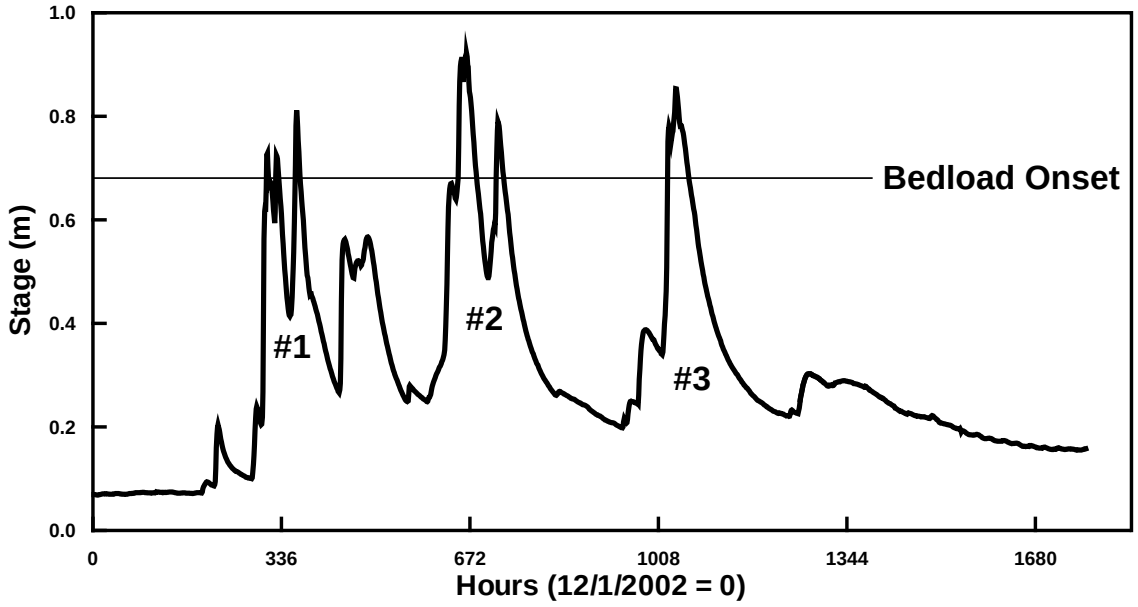

Figure 8. Hydrograph for Caspar Creek during events 1, 2 and 3.

At the Caspar Creek site, four 1/8 m3 bedload traps are enclosed in a concrete weir across a 4.4 m test channel. The trap boxes fit into vaults lined with rubber bumpers that center them over a load cell in the vault bottom. The vault tops have steel lids with a 100-mm (cross stream) by 400-mm opening through which bedload can fall. Training vanes along the slot sides prevent laterally-moving bedload from entering the traps. The trap openings are evenly spaced 0.71 m across the channel and comprise about 9% of its width.

Published online in 2010 as part of U.S. Geological Survey Scientific Investigations Report 2010-5091.

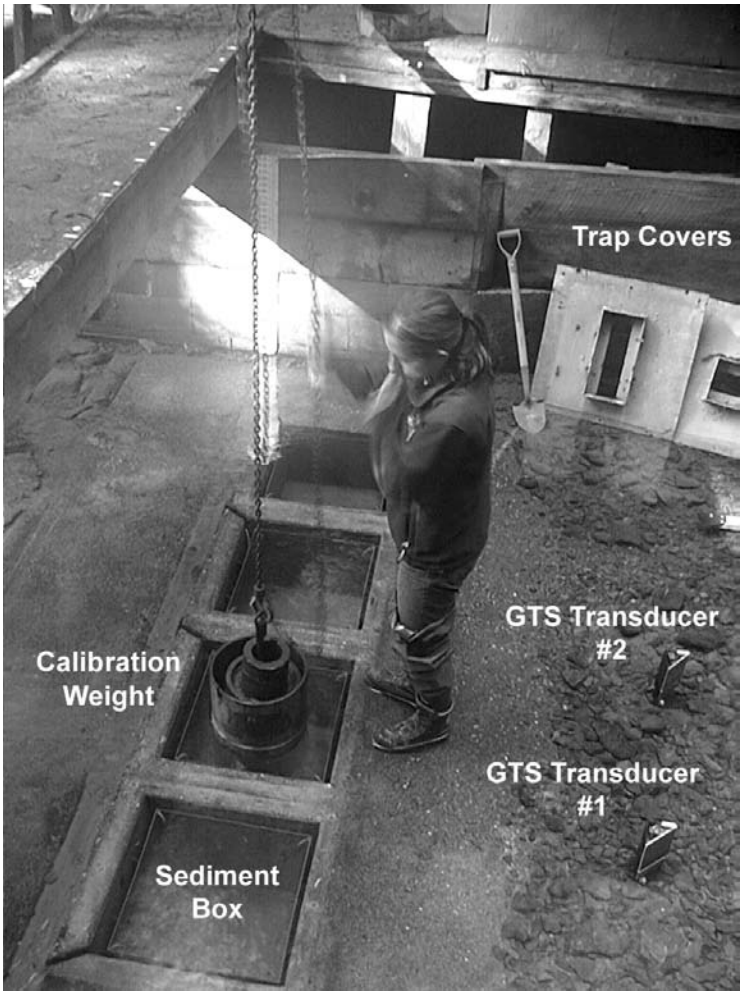

Figure 9. Caspar Creek installation.

The load-cells were calibrated onsite with weights placed in the boxes with a chain fall, Fig. 9. To calibrate, the boxes were loaded with calibration weights while the load-cell signals were recorded. Linear regressions of load-cell output signal on weight were computed and the resulting coefficients were entered into a CR10X data logger, enabling computation of time-stamped loads in kilograms six times per hour. The time series of trapped gravel mass was converted to momentum values so that factors could be developed to convert GTS data to mass transport. To do this, the gravel velocity had to be determined for the hydraulic conditions prevailing during each time step as described below.

4.1 Particle-Velocity Computations

In order to compare GTS and trap measurements, it is necessary to compute the velocities of trapped materials from stream hydraulics to obtain the total momentum which is adjusted for trap width and sampling time to determine the bedload momentum per channel width per time. Sekine and Kikkawa (1992) and Papanicolaou et al. (2002) provide an equation for computing saltation velocities from friction, critical-friction, and fall velocities. Critical-friction velocities were estimated using an equation given by Wilcock and Crowe (2003). Friction velocities were estimated using $U^* = (gsh)1/2$ and a record of local water depth and bed slope. Particle velocity was calculated with:

$$Up = \sqrt{Rgd}\left[1.7\frac{U*}{\omega}\sqrt{1-\frac{U*c}{U*}}+0.10\right]$$

where: g = gravitational acceleration; s = bed slope; h = water depth; R = relative submerged density (ρ_s-ρ)/ ρ; ρ = water density, ρ_s = sediment density (2650 kg m^{-3}); d = particle diameter; ω = fall velocity; U_* = friction velocity and U_{*c} = critical-friction velocity.

The size distribution of the gravel and its density were determined with a composite sample from the trap boxes. The sample was passed through a 4-mm sieve to recover the coarse material that the GTS could detect; this comprised about 47% of the bedload by weight. Next, the average density of the gravel was determined to be 2580 kg m-3 by measuring its volume and mass. Then, the sample was split into quarters and sized with a Gravelometer, a particle-size gauge available from Forestry Supply, Inc.

The size quartiles for the gravel are 7.2 mm (D25), 12 mm (D50), and 20 mm (D75). The threshold friction velocities were determined by the method of Wilcock and Crowe (2003) using a pebble count of the surface gravel on the delta immediately below the traps. The size quartiles for delta sediment were 3.2 mm, 9 mm, and 19 mm. The bed above the weir is coarser than the delta because it is armored and so critical friction and particle velocities may be lower than calculated.

The GTS stores time-stamped lines of pulse count (number of impact events), average pulse duration in μs, and average pulse area, μVs converted to digital counts. The sum of the products of pulse count and average pulse area over a measurement period is an estimate of the total momentum of gravel that impacted the transducers during that period. The conversion factor for the transducers is the ratio of the momentum of the trapped gravel and the counts recorded by the GTS, adjusted for the difference in the widths of the transducers and the trap openings.

4.2 Caspar Creek Results

Table 4 summarizes the results of the Caspar Creek tests. The first and third transport events (Fig. 8) produced conversion factors of 4.1 and 4.9 X 10-7 kg m s-1 per count respectively. Event-2 was the largest one during WY2003 with an average transport rate exceeding 21 kg m-1 h-1 before the boxes were filled. However, no conversion factor was determined because the GTS system was not turned on by the site attendant. The average transport rate during Event-3 was 18.4 kg m-1 h-1. There was bedload movement during subsequent events but the trap loads were less than 2 kg and the logger did not switch to the fast-sampling rate and acquire data.

Table 4. Summary of Casper Creek statistics.

Event	Duration (hours)	Mass (kg)	Ave. Qb (kg m^{-1} h^{-1})	P (kg m/s)	Counts (X 10^{-6})	CF (X 10^{7})
Event-1 (12/13-17/2002)	58	26.8	4.62	9.26	22.80	4.06
Event-2 (12/27-31/2002)	59	122	20.7	n.d.	n.d.	n.d.
Event-3 (1/12-13/2003)	40	73.5	18.4	27.80	58.10	4.79
Total transport hours	**157**					

.

5. Discussion

The conversion factors for the flume and field tests are different because the electronic gains of the signal-processors were set to different values. Moreover, the flume tests indicate that they are

proportional to bedload size. The efficiency (see Section 3) is degraded by the scour crater and mound that forms around a transducer which diverts some particles away from the pressure plate. A number of other particle motions that affect efficiency were observed but not quantified. They include: 1) particles can bounce along the pressure plate, producing multiple impacts, before being swept past it; 2) collateral impacts occur when dislodged particle strike the plate; and 3) particles near the plate vibrate in flow turbulence and produce spurious multiple contacts. These phenomena produce a positive bias in the detected momentum with an unknown magnitude. The aggregate effect of all biases could be substantial, and until more extensive calibration of this type is completed and the transducers are fully characterized for a range of size distributions, one must assume the uncertainty to be large.

In addition to the intrinsic uncertainty about efficiency and conversion factors, the results of the tests demonstrated several limitations to GTS use. The primary limitation is that the size distribution of the bedload must be known and must remain the same during a transport event. Several field studies have shown this not to be the case, and therefore even when the conversion factor is known, the errors associated with converting impact counts and average pulse areas to momentum can be large (Section 2.1). For example, bed-load-size fluctuations during transport events could cause standard errors in estimated particle velocities and mass transport as large as 100%. Another limitation is low efficiency. There is no easy remedy for this because smaller shapes, which presumably would be more efficient, are more fragile and sample less flow cross section than the present design. In other words, it is unclear whether the performance benefit would justify the reliability sacrifice. There are also limitations imposed by the high cross-channel variability of transport and the potentially large fluctuations in bed elevation in many streams that make total transport measurements with GTS-II systems impractical. In the former situation, an operator would have to maintain a prohibitively large array of embedded systems and many of them could be either buried or scoured from the bed. Measurements near structures such as culverts, bridge piers, and retaining walls as well as near stationary bed forms with relatively stable bed elevations are possible. The GTS-I is limited to streams with bridge access, water depths less than ~ 1.5 m, mean flow velocities less than 1.5 m s-1, well-sorted beds or beds with known load size distributions.

With minor engineering refinements of system packaging, circuit-board layout, and operator controls, the GTS designs described here are ready to be manufactured and used in beta tests at research sites. Because of the uncertainties associated with transducer efficiency, it is recommended that supporting hydraulic data, bedload samples, spot measurements with bedload traps be obtained. In 2008, the selling price of the Type I GTS is estimated to be $4,000 (USD) and the estimated price of the Type II GTS is $4,800.

6. Summary

1) Optimization of the detection circuit, filter shape, and threshold-detection scheme resulted in a minimum-detectable momentum of 0.0002 kg m s^{-1} (equivalent to a 5-mm stone moving at 0.12 m s^{-1}). Impact signals for spheres made of stone, glass, steel, and tungsten carbide, which have a wide range of mechanical properties showed no systematic variation in shape, amplitude or duration that could be attributed to particle mass. Estimation of particle mass from signal properties therefore appears to be unlikely.

2) GTS records of particle momentum can converted to mass transport with a method formulated on fractional particle speeds, settling and critical-shear velocities, and bed shear stress. The critical shear stress computation accounts for bed composition. Several published formulas can be used to calculate settling velocities and the bed shear stress can be estimated from local water depth and bed slope. With velocities estimated from stream hydraulics, the mass transport as bedload equals $P(\Sigma f_i V_{pi})^{-1}$, where: P

(momentum) equals digital counts multiplied by a conversion factor; f_i is the fraction of material in the i^{th} size class of the bedload size distribution; and V_{pi} is the velocity of the i^{th} size class.

3) The conversion factors for computing mass flux from GTS measurements were determined by comparing GTS data with values acquired with bedload traps in streams and with video images obtained in a flume. The factors determined from the flume tests were: 7.5, 9.9, and 12.6 mg m^{-1} s^{-1} per count for 13.4, 21.4, and 40-mm gravel respectively. The conversion factors determined for Caspar Creek data were 0.41 and 0.48 mg m^{-1} s^{-1} per count. Conversion factors vary from one instrument to another because of electronic gain and bedload size. Video analysis indicated that transducer efficiencies were about 20 to 40%, however, they were not correlated with particle size. Fast-moving particles made a disproportionately higher contribution to momentum measured in the flume than slow-moving ones.

4) Low transducer efficiency, < 50%, is a concern with the present design and can produce significant measurement errors. The inherent assumption in calculations of mass transport limits GTS use to streams with known bedload size distributions. High cross-channel variability in transport rates and system mortality resulting from bed-elevation fluctuations preclude the use of GTS-II systems for total load measurements, however, local measurements near stable bed forms and structures are possible. The 2008 costs of the current designs range from $4,000 to $4,800.

Acknowledgements

Development and testing of the GTS was supported by U.S. Department of Agriculture Small Business Innovation Research Program, Award Number 2001-33610-11233. I am grateful to Rand Eads (formerly with the USFS and now with Rivermetrics, Inc.), Jack Lewis and Liz Keppeler, U. S. Forest Service, Redwood Sciences Laboratory, Arcata, California for generous assistance with the Caspar Creek site from 1997 to 2003.

References

Bunte, K. I., Abt, S. R. & Potyondy, J. P. 2001. Portable bedload traps with high sampling intensity for representative sampling of gravel Transport in wadable mountain streams. In: *Federal Interagency Sedimentation* (Proc. Seventh Conf., Reno, Nevada, USA, March 2001), III-24–III-31.

Downing, J.P. 1981. ***Particle Counter for Sediment Transport Studies***. Journal of the Hydraulics Division, ASCE. Vol. HY11, pp. 1455-1465.

Downing, J. P. 1993. Particle Sensor for Stream Bed. U.S. Patent Number 5,207,090.

Downing, J. P. 2003. Particle momentum sensor. US Patent Number 6,601,464.

Downing, J., Farley, P., Bunte, K., Swingle, K., Ryan, S.E. and Dixon, M.. 2003. ***Acoustic gravel-transport sensor: description and field tests in Little Granite Creek, Wyoming, USA.*** Erosion and Sediment Transport Measurement in Rivers: Technological and Methodological Advances (ed. by J. Bogen, T. Fergus & D. E. Walling) pp. 193-200.

Downing, J., 2004. ***Acoustic Gravel-transport Sensor.*** Phase II Final report submitted to: United States Department of Agriculture Cooperative State Research, Education, and Extension Service Small Business Innovation Research Program.

Papanicolaou, A., Knapp, D and Strom, K. ***Bed load predictions by using the concept of particle velocity: Applications***. In: Proceedings of the ASCE/EWRI and IAHR International Conference on Hydraulic Measurements and Experimental Methods, July 2002, Estes Park, CO.

Sekine, M. and Kikkawa, H. 1992. ***Mechanics of Saltating Grains. II***. Journal of Hydraulic Engineering. Vol. 118, No. 4, pp. 536–558.

Sharp, B.B. and O'Niell, K.C., 1968. A new technique for discrete particle study in turbulent flow. In: *Proceedings of the Third Australasian Conference on Hydraulics and Fluid Mechanics. Sydney, Australia.*

Wilcock, P.R . and Crowe, J.C.. 2003. ***A Surface-based transport model for sand and gravel.*** Journal of Hydraulic Engineering. 129(2), pp. 120-128.